# Density functional study of hydrogen exchange and methane elimination from bis(cyclopentadienyl)tungsten methyl hydrides and their *ansa*-bridged analogues

**Jennifer C. Green and Christian N. Jardine**

*Inorganic Chemistry Laboratory, South Parks Road, Oxford, UK OX1 3QR*

Theoretical calculations have been carried out using density functional theory on the hydrogen exchange and methane elimination reactions of $[W(\eta\text{-}C_5H_5)_2(Me)H]$ and $[W\{(\eta\text{-}C_5H_4)_2CH_2\}(Me)H]$. In both cases the hydrogen exchange proceeds along a similar reaction path on which lies a $\eta^1$-H $\sigma$ complex. The midpoint of the exchange reaction is a $\eta^2$-H,H $\sigma$ complex. For $[W(\eta\text{-}C_5H_5)_2(Me)H]$ a transition state is proposed which is calculated to lie 81 kJ mol$^{-1}$ above the ground state. This compares with an experimental free energy of activation of 106 kJ mol$^{-1}$ for $[W(\eta\text{-}C_5H_5)_2(Me)D]$. Elimination of methane is calculated to have an overall reaction energy of 19.6 kJ mol$^{-1}$ for $[W(\eta\text{-}C_5H_5)_2(Me)H]$ and 78.3 kJ mol$^{-1}$ for $[W\{(\eta\text{-}C_5H_4)_2CH_2\}(Me)H]$. The activation energy for elimination from the two compounds is estimated as around 80 and 85 kJ mol$^{-1}$ respectively. The principal reason for the relative stability of the $[W(\eta\text{-}C_5H_5)_2]$ product is its relaxation to a parallel ring triplet state which is calculated to lie 67.9 kJ mol$^{-1}$ below the lowest excited singlet state. For $[W\{(\eta\text{-}C_5H_4)_2CH_2\}]$ the singlet and triplet states are separated by 13.3 kJ mol$^{-1}$ with the rings inclined at an angle constrained by the *ansa* bridge.

Bis(cyclopentadienyl)tungsten, $[W(\eta\text{-}C_5H_5)_2]$, is a well characterised unstable intermediate [1,2] with the capacity to activate C–H bonds.[3–6] It may be formed by solution photolysis of $[W(\eta\text{-}C_5H_5)_2H_2]$ or $[W(\eta\text{-}C_5H_5)_2(CO)]$; elimination of $H_2$ or CO occurs and the $[W(\eta\text{-}C_5H_5)_2]$ moiety inserts into the alkyl or aryl C–H bonds of substrates such as benzene, mesitylene or tetramethylsilane.[4–6] Thermolysis of $[W(\eta\text{-}C_5H_5)_2(Me)H]$ results in elimination of $CH_4$ and generation of almost identical products implying the same $[W(\eta\text{-}C_5H_5)_2]$ intermediate.[4] The reverse of this reaction, namely the activation of methane by $[W(\eta\text{-}C_5H_5)_2]$, has not been reported.

A thorough and elegant study of the elimination of methane from $[W(\eta\text{-}C_5H_5)_2(Me)H]$ has been carried out by Norton and co-workers.[7,8] In the presence of acetonitrile as a trapping agent for $[W(\eta\text{-}C_5H_5)_2]$, and in dilute solution, methane elimination was found to be intramolecular. Elimination of methane shows an inverse kinetic isotope effect, equation (1). At 48 °C
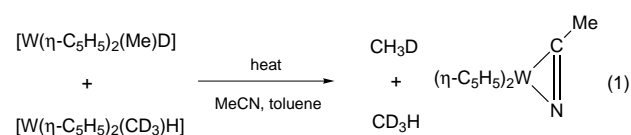


$[W(\eta\text{-}C_5H_5)_2(Me)D]$ showed hydrogen exchange between the alkyl and hydride, equation (2). The equilibrium constant is 1.4,
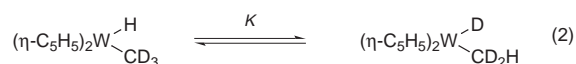


less than the statistical value of 3.0 because the difference between the C–H and C–D zero-point energy is greater than that between the W–H and W–D zero-point energies.[8]

In solutions of concentration greater than 0.01 M isotopically labelled species of $[W(\eta\text{-}C_5H_5)_2(Me)H]$ underwent label scrambling by an intermolecular mechanism prior to methane elimination.[8] The rate constant for intramolecular scrambling alone is $2.5 \times 10^{-5}$ s$^{-1}$ and is independent of concentration. The activation energies for hydrogen exchange and methane elimination are 25.4 and 26.4 kcal mol$^{-1}$ (106 and 110 kJ mol$^{-1}$) respectively.

Studies on $[W(\eta\text{-}C_5Me_5)_2(Me)D]$ and $[W(\eta\text{-}C_5Me_5)_2(CD_3)H]$ also show hydrogen exchange and methane elimination reactions.[9] Both exhibit an inverse kinetic isotope effect; however, in this case the elimination occurs faster than the exchange reaction.

The *ansa*-bridged compound $[W\{(\eta\text{-}C_5H_4)_2CMe_2\}(Me)H]$ first made by Labella *et al.*[10] was found to be stable toward reductive elimination of methane under both photochemical and thermal conditions. It is stable up to 120 °C whereas the unbridged analogue decomposes slowly at 48 °C. This unusual stability was attributed to the inability of the proposed 16-electron intermediate $[W\{(\eta\text{-}C_5H_4)_2CMe_2\}]$ to adopt a parallel ring structure which is the ground state for $[W(\eta\text{-}C_5H_5)_2]$. Souter and co-workers [11] demonstrated that scrambling of $[W\{(\eta\text{-}C_5H_4)_2CMe_2\}(Me)H]$ occurs *via* an intramolecular mechanism in both concentrated and dilute solution.

In a similar fashion $[W\{(\eta\text{-}C_5H_4)_2CMe_2\}H_2]$ is photochemically inert in contrast to the activity of the unbridged analogue described above.[10] Munakata [12] has calculated the energetics involved in various photochemical pathways and concludes the difference is due to the relative stability of the triplet tungstenocene with parallel rings. Brintzinger *et al.*[13] also discussed the photochemical elimination of $H_2$ from $[W(\eta\text{-}C_5H_5)_2H_2]$ in these terms.

Detailed studies on the alkyl hydride complexes $[Rh(\eta\text{-}C_5Me_5)(PMe_3)(Et)D]$ and $[Ir(\eta\text{-}C_5Me_5)(PMe_3)(C_6H_{11})D]$ have also been performed by Bergmann and co-workers [14,15] in order to elucidate the mechanisms responsible for H/D exchange and alkane elimination.

There is a general consensus that both exchange and elimination reactions found for these alkyl hydrides proceed through a $\sigma$-complex intermediate.[16,17] The symmetry of the exchange pathway implies at some stage a $\eta^2$-H,H structure **I** where both hydrogens are equidistant from the metal. Elimination can, however, occur through a $\eta^2$-H,C structure or $\eta^1$-H structure **II**.
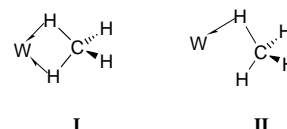
**Table 1** Summary of calculations carried out and geometric constraints

| Calculation type | Structure | Symmetry |
|---|---|---|
| Geometry optimisation and frequency | $[W(\eta\text{-}C_5H_5)_2(Me)H]$ | None |
| Geometry optimisation and frequency | $[W(\eta\text{-}C_5H_5)_2(CH_4)] (\eta^2\text{-}H,H)$ | $C_{2v}$ |
| Geometry optimisation | $[W(\eta\text{-}C_5H_5)_2(CH_4)] (\eta^2\text{-}H,H)$ | $C_2$ |
| Geometry optimisation | $[W(\eta\text{-}C_5H_5)_2(CH_4)] (\eta^2\text{-}H,H)$ | $C_s$ |
| Geometry optimisation and frequency | $[W(\eta\text{-}C_5H_5)_2(CH_4)] (\eta^1\text{-}C,H)$ | None |
| Linear transit (C–H 1.125–2.582 Å) | $[W(\eta\text{-}C_5H_5)_2(CH_4)]$ to $[W(\eta\text{-}C_5H_5)_2(Me)H]$ | None |
| Geometry optimisation and frequency * | $[W(\eta\text{-}C_5H_5)_2]$ singlet | None |
| Geometry optimisation and frequency * | $[W(\eta\text{-}C_5H_5)_2]$ triplet | None |
| Linear transit (W–C 2.25–4.5 Å) | $[W(\eta\text{-}C_5H_5)_2(CH_4)]$ singlet | $C_{2v}$ |
| Linear transit (W–C 3.0–5.0 Å) | $[W(\eta\text{-}C_5H_5)_2(CH_4)]$ triplet | $C_{2v}$ |
| Geometry optimisation | $[W\{(\eta\text{-}C_5H_4)_2CH_2\}(Me)H]$ | None |
| Geometry optimisation | $[W\{(\eta\text{-}C_5H_4)_2CH_2\}(CH_4)] (\eta^2\text{-}H,H)$ | $C_{2v}$ |
| Geometry optimisation | $[W\{(\eta\text{-}C_5H_4)_2CH_2\}(CH_4)] (\eta^1\text{-}C,H)$ | None |
| Geometry optimisation | $[W\{(\eta\text{-}C_5H_4)_2CH_2\}]$ singlet | None |
| Geometry optimisation | $[W\{(\eta\text{-}C_5H_4)_2CH_2\}]$ triplet | None |
| Linear transit (W–C 2.25–4.5 Å) | $[W\{(\eta\text{-}C_5H_4)_2CH_2\}(CH_4)]$ singlet | $C_{2v}$ |
| Linear transit (W–C 3.5–5.0 Å) | $[W\{(\eta\text{-}C_5H_4)_2CH_2\}(CH_4)]$ triplet | $C_{2v}$ |

* Low negative frequencies were found for this optimised structure corresponding to relative rotation of the cyclopentadienyl rings.

Indeed the fact that elimination is faster than scrambling in $[W(\eta\text{-}C_5Me_5)_2(Me)H]$ suggests such a structure for elimination in this case.[9]

We report here theoretical calculations, using density functional theory, on ground states, products and possible reaction pathways for exchange and elimination from both $[W(\eta\text{-}C_5H_5)_2(Me)H]$ and $[W\{(\eta\text{-}C_5H_4)_2CH_2\}(Me)H]$, as a model for $[W\{(\eta\text{-}C_5H_4)_2CMe_2\}(CD_3)H]$, in order to understand in more detail the effect of the *ansa* bridge on the reactivity of these compounds.

## Computational Details

All calculations were carried out using the Amsterdam density functional (ADF) program system.[18] The electronic configurations of the molecular systems were described by an uncontracted triple-$\zeta$ basis set of Slater-type orbitals (STOs). Hydrogens and carbons were given an extra polarisation function, 2p on H and 3d on C. The cores of the atoms were frozen, C up to 1s and W up to 5p. First-order relativistic corrections were made to the cores of all atoms using the Pauli formalism.

Energies were calculated using Vosko, Wilk and Nusair's local exchange correlation potential[19] with non-local-exchange corrections by Becke[20] and non-local-correlation corrections by Perdew.[21,22] The non-local correction terms were utilised in calculating gradients during geometry optimisations. The calculations carried out are summarized in Table 1.

## Results and Discussion

### Ground-state structures

The structures of $[W(\eta\text{-}C_5H_5)_2(Me)H]$ and $[W\{(\eta\text{-}C_5H_4)_2CH_2\}(Me)H]$ were successfully optimised to the structures **1** and **2** under no symmetry constraints. The input structure for the *ansa*-bridged species was taken from crystal data;[23] structure **2** gave bond lengths and angles differing by under 5%. The values are compared in Table 2. The relatively short distance to the bridgehead carbons of the cyclopentadienyl rings was reproduced by the calculation. The most significant difference between **1** and **2** is the smaller angle between the normals to the rings predicted for **2**. No structural data exist for $[W(\eta\text{-}C_5H_5)_2(Me)H]$ but ring–W–ring angles around 140° are typical for bis(cyclopentadienyl) compounds.
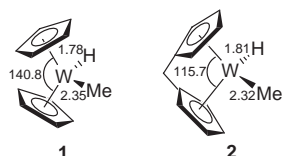


**Table 2** Selected bond lengths (Å) and angles (°) calculated for $[W\{(\eta\text{-}C_5H_4)_2CH_2\}(Me)H]$ and measured for $[W\{(\eta\text{-}C_5H_4)_2CMe_2\}(CD_3)H]$[23]

| Parameter | Calculated | Crystal Structure |
|---|---|---|
| W–C (methyl) | 2.32 | 2.23 |
| W–H | 1.81 | |
| W–C ($C_5H_4$ ring) | 2.36–2.49 | 2.22–2.35 |
| C–C ($C_5H_4$ ring) | 1.42–1.44 | 1.43–1.47 |
| C–W–H | 76 | |
| $C_5H_4$ normal–W–$C_5H_4$ normal | 115.7 | 119.9 |

### The hydrogen exchange pathway

Since the exchange pathway has a symmetric reaction profile, the exchanging hydrogens must be geometrically equivalent at the midpoint. Thus, the midpoint structure must contain a symmetry operation exchanging the two reacting hydrogens. The possibilities for the associated point groups are $C_{2v}$, $C_2$ and $C_s$. The preference of a bent bis(cyclopentadienyl) unit for bonding in the plane bisecting the ring–metal–ring angle suggests that the co-ordinating hydrogens will remain in the plane perpendicular to the ring normals. The overall symmetry of such a structure will depend on the ring orientations; if the rings are eclipsed in the manner that is forced on them by the *ansa* bridge the overall symmetry at the midpoint will be $C_{2v}$.
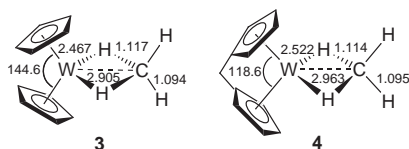
Proposed midpoints are either a dihydrido carbene, **III**, or a $\eta^2$-H,H methane complex, $[W(\eta\text{-}C_5H_5)_2(CH_4)]$ **IV**.
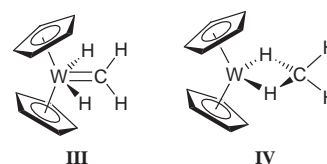


Optimisations were carried out on both $[W(\eta\text{-}C_5H_5)_2(CH_4)]$ and $[W\{(\eta\text{-}C_5H_4)_2CH_2\}(CH_4)]$ with various starting geometries with the constraint of $C_{2v}$ symmetry. To model the dihydrido carbene structures, starting distances of W–C at 2.27 Å and W–H at 1.67 Å and a C–W–H bond angle of 46.9° were used. From all initial geometries minimum energy structures **3** and **4** were found for the two complexes. Structural details are given in Table 3. The C–H (exchanging) bond length is computed in both cases to be slightly longer than the C–H (non-exchanging) distance reflecting the $\eta^2$-H,H character of these species. Overall methane appears to be bound slightly more weakly in the *ansa*-bridged complex than in the unbridged one.

**Table 3** Structural parameters (bond lengths in Å, angles in °) calculated for the minimum-energy structures of $[W(\eta\text{-}C_5H_5)_2(CH_4)]$ and $[W\{(\eta\text{-}C_5H_4)_2CH_2\}(CH_4)]$ constrained to $C_{2v}$ symmetry

| Parameter | $[W(\eta\text{-}C_5H_5)_2(CH_4)]$ | $[W\{(\eta\text{-}C_5H_4)_2CH_2\}(CH_4)]$ |
| --- | --- | --- |
| W–H | 2.467 | 2.522 |
| W–C | 2.905 | 2.963 |
| C–H (exchanging) | 1.117 | 1.114 |
| (non-exchanging) | 1.094 | 1.095 |
| ring–W–ring | 144.6 | 118.6 |
| (normals) | | |
| W–C (ring) | 2.34–2.39 | 2.28–2.42 |
| C–C (ring) | 1.43–1.45 | 1.43–1.46 |



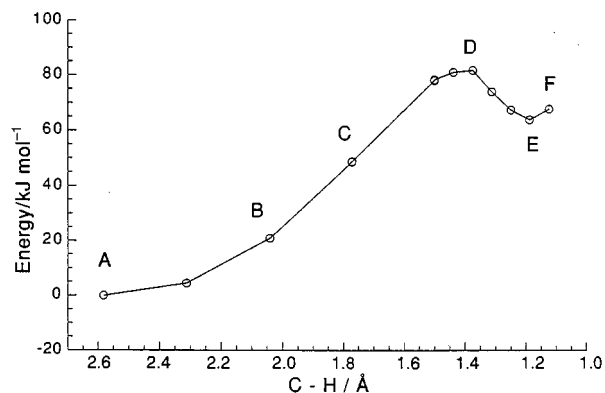**Fig. 1** Variation in energy found for proposed reaction pathway between complexes **1** and **3**



The structure of $[W(\eta\text{-}C_5H_5)_2(CH_4)]$ was also optimised with both $C_s$ and $C_2$ symmetry constraints. Local minima were found in both symmetries. With $C_s$ symmetry the W–C and W–H distances were longer by 0.05 Å and the energy higher by 0.03 eV (2.89 kJ mol$^{-1}$). With $C_2$ symmetry the methane was twisted by 7.8° and again the energy was higher this time by 0.02 eV (2.02 kJ mol$^{-1}$).

A frequency test on the $C_{2v}$ species reveals two imaginary frequencies of $B_2$ symmetry at 231.07 and 68.45$i$ cm$^{-1}$ ($i = \sqrt{-1}$). The former vibration is a rotation of the methane unit relative to the $[W(\eta\text{-}C_5H_5)_2]$ fragment and moves one H closer to the metal and the other further away, **V**. The latter is a swinging motion of the methyl group in the mirror plane containing the two hydrogens relative to the rings, thus the C moves off the two-fold axis, **VI**. A combination of these two vibrations would convert the $\eta^2$-H,H σ complex **I** into a $\eta^1$-H σ complex **II**. It also suggests that a lower-energy structure could be achieved with a slightly different ring orientation.
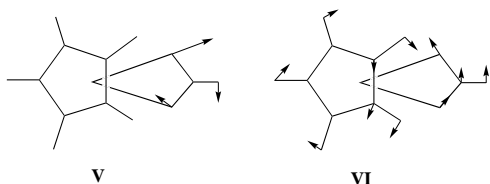


A sequence of geometry optimisations (linear transit run) was carried out in which the distance between C and the migrating hydrogen was constrained to a series of values representing breaking of the C–H bond. The starting structure was the $C_{2v}$ optimised geometry for $[W(\eta\text{-}C_5H_5)_2(CH_4)]$ **3**, and the final distance corresponded to that found for $[W(\eta\text{-}C_5H_5)_2(Me)H]$. The geometry found for the final structure was very similar to that of **1**. The energy profile found is shown in Fig. 1. Diagrams of the structures found at six points on the linear transit run are shown in Fig. 2. The variations found from **A** to **C** are principally in the C–H distance and H–W–C angle and the motion resembles a bending vibration. By **D** the W–H has lengthened, and the C–H bond has not yet formed, but the methyl group has turned towards the approaching hydrogen. Structure **D** lies 81 kJ mol$^{-1}$ above **A**. Structure **E**, which is at the shallow dip of the reaction coordinate, has features of a $\eta^1$-H σ complex and **F** is **3** the $C_{2v}$ $\eta^2$-H,H complex.

As structure **E** appeared as a minimum on the reaction profile, lying 4 kJ mol$^{-1}$ below **F**, a geometry optimisation was attempted with this as the starting structure. A minimum was found with energy and bond parameters very close to those of **E**. These are shown in the representation of the $\eta^1$-H σ com-
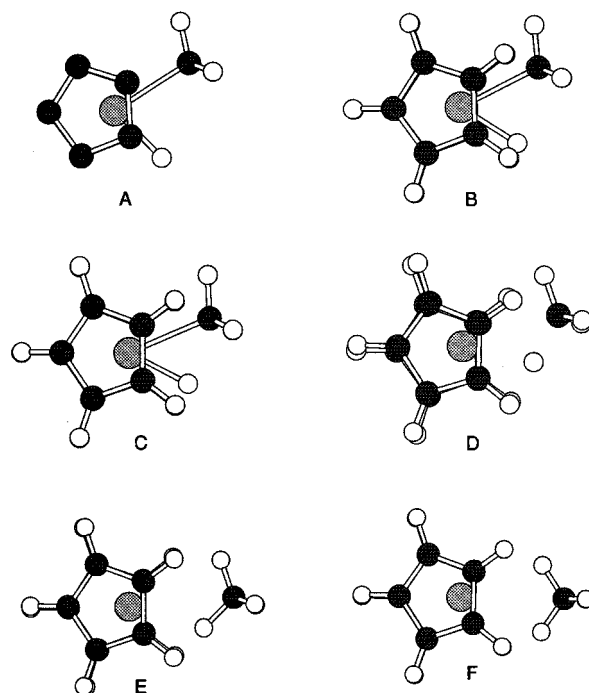
**Fig. 2** Structures found for six points **A**–**F** on the linear transit run: **A** is the ground-state structure found for complex **1** (the cyclopentadienyl hydrogens are omitted as they obscure the tungsten hydride), **D** represents the maximum energy point and **E** a minimum close to the $C_{2v}$ structure which is represented by **F**

plexes, **5** and **6**. A vibrational calculation showed all frequencies to be real and demonstrated that this was a local minimum. The similarity of W–C distances between **3** and **5** and between **4** and **6** lead us to classify **5** and **6** as $\eta^1$-H rather than $\eta^2$-C,H σ complexes. The closeness of **E** to **F** in energy, and the proximity of the optimised $C_s$ and $C_2$ structures, all suggest that the midpoint of the exchange reaction must lie very close to **F**. Though we were unable to locate the transition state at the midpoint it seems likely that the W(CH$_4$) fragment has $C_{2v}$ symmetry but the rings are oriented so as to break that symmetry.
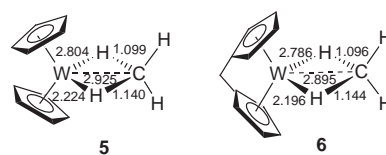


**Methane loss**

For computational simplicity the loss of methane was most easily modelled with the constraint of $C_{2v}$ symmetry. The small
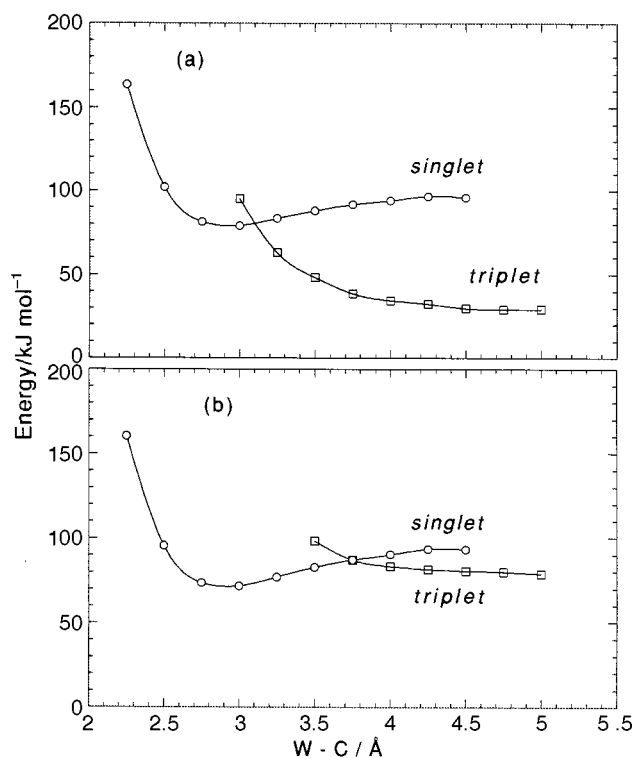
**Fig. 3** Energies of triplet and singlet $C_{2v}$ methane complexes (a) [W(η-C$_5$H$_5$)$_2$(CH$_4$)] and (b) [W{(η-C$_5$H$_4$)$_2$CH$_2$}(CH$_4$)] at varying W–C distance with respect to the energy of the corresponding methyl hydride

energy difference found between the η$^1$-H and η$^2$-H,H structures revealed by the exchange study suggests that the approximation involved is trivial.

The loss of methane from [W(η-C$_5$H$_5$)$_2$(CH$_4$)] and [W{(η-C$_5$H$_4$)$_2$CH$_2$}(CH$_4$)] was modelled by utilising the W–C distance as a reaction coordinate, and optimising the molecular geometry, while varying the W–C distance from 2.25 to 5.0 Å. The symmetry was constrained to $C_{2v}$ throughout. The energy profile showed a potential well for both systems, illustrated in Fig. 3. The η$^2$-H,H structures lay at the bottom of their respective potential wells. Thus, for both compounds, there appears to be a greater barrier to methane elimination than there is to hydrogen exchange.

Geometry optimisations of the free singlet tungstenocenes were performed under no geometry constraints, finding minima at structures **7** and **8**. The depth of the potential well was calculated by subtracting the energy of the σ complex from that of the free singlet metallocene plus that of CH$_4$. This gave a well depth for the bridged and non-bridged systems of 0.246 and 0.195 eV (23.74 and 18.81 kJ mol$^{-1}$) respectively. The overall energy required to form CH$_4$ and singlet tungstenocene from the methyl hydride is 0.949 eV (91.52 kJ mol$^{-1}$) for the bridged system and 0.907 eV (87.51 kJ mol$^{-1}$) for the *ansa*-bridged. Such similar values are at odds with the experimental observation that the *ansa*-bridged complex is thermally stable whereas the non-bridged complex decomposes readily on heating.
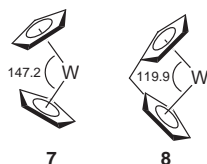


Infrared and UV matrix-isolation studies[2] have shown [W(η-C$_5$H$_5$)$_2$] to have a parallel sandwich structure with a $^3E_2$ ground state. Geometry optimisations were performed on the non-bridged and *ansa*-bridged tungstenocenes in the triplet state showing minima corresponding to structures **9** and **10**. The

optimisation predicts the non-bridged tungstenocene to have a ring angle of 172.1° due to a Jahn–Teller distortion, analogous to that found in molybdenocene.[2] However, it has been shown that this is quenched in tungstenocene by spin–orbit coupling, and the rings are parallel in the ground-state structure.[2]
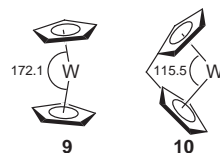


For [W(η-C$_5$H$_5$)$_2$] the triplet state is calculated to lie 0.704 eV (67.9 kJ mol$^{-1}$) below the singlet state. In the case of [W{(η-C$_5$H$_4$)$_2$CH$_2$}] the triplet is again lower in energy, but the difference is considerably less being calculated as only 0.138 eV (13.3 kJ mol$^{-1}$). Taking into account the likely triplet nature of the metallocene products, the overall reaction energies are 0.230 eV (19.6 kJ mol$^{-1}$) for [W(η-C$_5$H$_5$)$_2$(Me)H] and 0.811 eV (78.3 kJ mol$^{-1}$) for [W{(η-C$_5$H$_4$)$_2$CH$_2$}(Me)H]. It is this difference in reaction enthalpies that enables the thermal elimination of methane to occur at a much lower temperature for [W(η-C$_5$H$_5$)$_2$(Me)H] than for [W{(η-C$_5$H$_4$)$_2$CH$_2$}(Me)H].

Energy profiles were elucidated for the triplet states of both systems, again using the W–C distance as a reaction coordinate and constraining the system to $C_{2v}$ symmetry (Fig. 3). They both show a decay in energy with increasing W–C distance, but the contrast between the bridged and unbridged systems is much greater. As methane moves away the lowering of energy for the unbridged system is associated with triplet [W(η-C$_5$H$_5$)$_2$] relaxing to a parallel ring structure. Relatively little energy gain is possible on forming the triplet in the case of [W{(η-C$_5$H$_4$)$_2$CH$_2$}(Me)H] as the rings are constrained by the bridge.

Fig. 3(a) shows the singlet and triplet curves of the unbridged system crossing at a W–C distance of 3.1 Å. However, both these curves represent optimum geometries for the triplet and singlet systems given the one constraint of fixed W–C distance, so other geometrical parameters are likely to be different and this point does not represent the exact singlet–triplet crossover. Examination of the optimised geometries at this distance suggests that the most significant structural difference between the singlet and triplet is the ring–metal–ring angle, which for the singlet state is 14° less than for the triplet state.

Vibrational frequency analysis on the singlet [W(η-C$_5$H$_5$)$_2$(CH$_4$)] complex shows that the ring bending is a very loose motion (99.4 cm$^{-1}$), and thus attaining a suitable structure for singlet–triplet crossover will be facile, and the crossover point shown in Fig. 3(a) probably represents a close approximation to the critical W–C distance for the crossover. It lies *ca.* 0.05 eV above the minimum in the potential well.

Conversely the *ansa*-bridged rings must move through only 3° to cross to the triplet state, but this is counteracted by the rigidity of the motion. More crucially, it is only energetically viable to access the triplet surface at greater W–C distances [Fig. 3(b)]. Thus, a more extreme geometric change is required for *ansa*-bridged species before the triplet state may be adopted. The lateness of this transition state will provide a kinetic barrier to loss of methane.

Furthermore, it has been observed by Parkin and Bercaw[9] that the rate of elimination of methane from [W(η-C$_5$Me$_5$)$_2$(Me)H] is faster than the hydrogen exchange process. We postulate that, for this system, the loss of methane is also driven by conversion into a triplet parallel sandwich structure, permethyltungstenocene. The steric bulk of the methyl groups on the cyclopentadienyl rings flattens the ring angle of the methyl hydride facilitating singlet–triplet crossover at smaller W–C distances than in the [W(η-C$_5$H$_5$)$_2$(Me)H] analogue. Thus, the transition state for singlet–triplet crossover will be at lower energy and more accessible than that for hydrogen exchange.
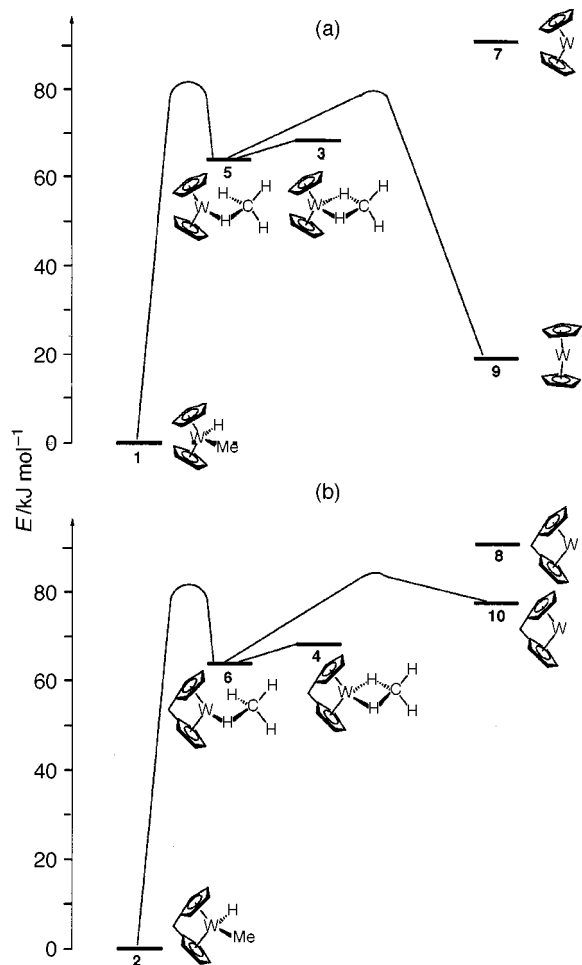
**Fig. 4** Energy scheme for hydrogen exchange and methane elimination: (a) [W($\eta$-C$_5$H$_5$)$_2$(Me)H] and (b) [W{($\eta$-C$_5$H$_4$)$_2$CH$_2$}(Me)H]

A combined energy scheme for exchange and elimination for both systems is shown in Fig. 4. The activation energies for elimination are estimated as *ca.* 80 and 85 kJ mol$^{-1}$ for the unbridged and *ansa*-bridged compounds respectively.

It is of interest to consider the implications of the energetics found for elimination in the context of the reverse reaction, alkane activation. Given that alkane activation is unfavourable entropically, the high activation energy of *ca.* 60 kJ mol$^{-1}$ and small overall energy gain of *ca.* −20 kJ mol$^{-1}$ predicted when

tungstenocene is the reactant seem to inhibit the activation. However, when tungstenocene is preorganised into a bent state by linking the two rings with an *ansa* bridge the activation energy is reduced to *ca.* 10 kJ mol$^{-1}$ and there is a much higher energy gain of *ca.* −80 kJ mol$^{-1}$; this could well mean that such a reaction is favoured. Chemical generation of *ansa*-bridged tungstenocene thus presents itself as an interesting synthetic target.

## References

1 P. Grebnik, A. J. Downs, M. L. H. Green and R. N. Perutz, *J. Chem. Soc., Chem. Commun.*, 1979, 742.
2 J. Chetwynd-Talbot, P. Grebnik and R. N. Perutz, *Inorg. Chem.*, 1982, **21**, 3647.
3 C. Gianotti and M. L. H. Green, *J. Chem. Soc., Chem. Commun.*, 1972, 1114.
4 N. J. Cooper, M. L. H. Green and R. Mahtab, *J. Chem. Soc., Dalton Trans.*, 1979, 1557.
5 M. Berry, K. Elmitt and M. L. H. Green, *J. Chem. Soc., Dalton Trans.*, 1979, 1950.
6 M. Berry, N. J. Cooper, M. L. H. Green and S. J. Simpson, *J. Chem. Soc., Dalton Trans.*, 1980, 29.
7 R. M. Bullock, C. E. L. Headford, S. E. Kegley and J. R. Norton, *J. Am. Chem. Soc.*, 1985, **107**, 727.
8 R. M. Bullock, C. E. L. Headford, K. M. Hennessy, S. E. Kegley and J. R. Norton, *J. Am. Chem. Soc.*, 1989, **111**, 3897.
9 G. Parkin and J. E. Bercaw, *Organometallics*, 1989, **8**, 1172.
10 L. Labella, A. Chernega and M. L. H. Green, *J. Chem. Soc., Dalton Trans.*, 1995, 395.
11 A. Chernega, J. Cook, M. L. H. Green, L. Labella, S. J. Simpson, J. Souter and A. H. H. Stephens, *J. Chem. Soc., Dalton Trans.*, 1977, 3225.
12 H. Munakata, American Chemical Society, New Orleans, 1996.
13 H. H. Brintzinger, L. L. Lohr and K. L. Tang Wong, *J. Am. Chem. Soc.*, 1975, **97**, 5146.
14 R. A. Periana and R. G. Bergmann, *J. Am. Chem. Soc.*, 1986, **108**, 7332, 7346.
15 J. M. Buchanan, J. M. Stryker and R. G. Bergmann, *J. Am. Chem. Soc.*, 1986, **108**, 1537.
16 R. H. Crabtree, *Angew. Chem., Int. Ed. Engl.*, 1993, **32**, 789.
17 C. Hall and R. N. Perutz, *Chem. Rev.*, 1996, **96**, 3125.
18 ADF (version 2.0.1), G. te Velde and E. J. Baerends, Department of Theoretical Chemistry, Vrije Universiteit, 1996.
19 S. H. Vosko, L. Wilk and M. Nusair, *Can. J. Phys.*, 1980, **58**, 1200.
20 A. D. Becke, *Phys. Rev. A*, 1988, **38**, 2398.
21 J. P. Perdew, *Phys. Rev. B*, 1986, **33**, 8822.
22 J. P. Perdew, *Phys. Rev. B*, 1986, **34**, 7046.
23 J. Souter, D.Phil. Thesis, University of Oxford, 1996.